



**Measurement of the $t\bar{t}$ production cross section
in $p\bar{p}$ collisions at $\sqrt{s} = 1.96$ TeV
in the multi-jet final state**

The DØ Collaboration
URL <http://www-d0.fnal.gov>
(Dated: March 22, 2006)

The cross section for the production of pairs of top quarks was measured in high-multiplicity jet events. The top-quark signal was extracted using the combination of identified b jets and W bosons reconstructed from dijets. The cross section was 12.1 ± 4.9 (stat.) ± 4.6 (sys.) pb assuming $m_t = 175$ GeV and is consistent with the Standard Model expectation.

The top quark is the heaviest known fundamental particle and measurements of its production rate allow for precision tests of quantum chromodynamics (QCD). This paper describes a measurement by the DØ collaboration of the $t\bar{t}$ production cross section in $p\bar{p}$ collisions at $\sqrt{s} = 1.96$ TeV at the Fermilab Tevatron Collider. The top quark is primarily produced in pairs at the Tevatron and decays to a W boson and b quark with a branching ratio of $\approx 100\%$ within the Standard Model. The W boson subsequently decays into a lepton–neutrino or a quark–anti-quark pair. Top events are classified according to this W boson decay channel. The multi-jet decay mode, the focus of this study, includes contributions from the all-hadronic channel (both W bosons decay to quarks), the τ channels when the τ decays hadronically, and the other decay channels when additional jets are produced.

The DØ detector has a central-tracking system, consisting of a silicon microstrip tracker and a central fiber tracker, both located within a 2 T superconducting solenoidal magnet [1], with designs optimized for tracking and vertexing at pseudorapidities $|\eta| < 3$ and $|\eta| < 2.5$, respectively. A liquid-argon and uranium calorimeter has a central section covering pseudorapidities $|\eta|$ up to ≈ 1.1 , and two end calorimeters (EC) that extend coverage to $|\eta| \approx 4.2$, with all three housed in separate cryostats [2]. An outer muon system, at $|\eta| < 2$, consists of a layer of tracking detectors and scintillation trigger counters in front of 1.8 T toroids, followed by two similar layers after the toroids [3]. Luminosity is measured using plastic scintillator arrays placed in front of the EC cryostats. The trigger and data acquisition systems are designed to accommodate the high luminosities of Run II at the Fermilab Tevatron Collider.

The data considered in this analysis were acquired using multi-jet triggers with a total integrated luminosity of $\mathcal{L} = 360 \pm 24 \text{ pb}^{-1}$ [4]. Data selection was based on run quality, event properties, and jet quality criteria. Events were required to have a primary vertex, formed from at least 3 tracks, reconstructed within 50 cm of the nominal center of the detector. Calorimeter-based jets were reconstructed using the Run II mid-point cone algorithm with cone radius 0.5 [5]. Backgrounds from multiple interactions were suppressed by requiring jets to have at least two tracks, reconstructed within the jet cone, that pointed to the primary vertex. Events were required to have six jets with at least two jets having $p_T > 45$ GeV, two other jets having $p_T > 20$ GeV, and the rest having $p_T > 15$ GeV. All jets were required to be within $|y| < 2.4$. No event vetoes were applied for high- p_T leptons or E_T .

Candidate $t\bar{t}$ events required at least two jets with $p_T > 45$ GeV tagged as b jets with the secondary vertex tagger (SVT) [6] algorithm. The other jets were required not to be identified as b -tagged jets by this definition. This is the “loose” event sample. The dijet mass distribution (two non- b tagged jets) and the three-jet mass distribution ($bjj =$ one b -tagged jet and two non- b tagged jets) are shown in Fig. 1. All possible combinations of jets were entered into each mass distribution. Excursions are visible in the dijet mass distribution near the mass of the W boson and in the bjj mass distribution near the top-quark mass. Two additional samples, “medium” and “tight”, with requirements on topological variables, were considered for systematic studies (Table I). Cuts on aplanarity (\mathcal{A}), centrality (\mathcal{C}), sphericity (\mathcal{S}), and the ΔR between the two b jets ($\Delta R_{b\bar{b}}$) were used to enhance top-like events.

The identification of the b jet from the top decay was used to suppress the multi-jet backgrounds that otherwise obfuscate $t\bar{t}$ production at the Tevatron. Distributions representing the background, primarily due to multi-jet QCD production and electroweak W boson production with associated jets, were derived from the data. Two jets in each event were chosen at random and defined to be b jets irrespective of their actual tag status. Background events were otherwise treated in the same manner as the candidates, including the requirements on the b and non- b jets.

Kinematic correlations between b -tagged jets were not completely modeled by the random multi-jet sample, therefore two weights were applied to the jets in the background sample. One was based on the b -tagged jet p_T spectrum and the other on the angular correlation between the two b -tagged jets (ΔR_{bb}). The p_T -dependent per-jet weight was derived from a sample of tagged jets depleted in real b jets. A four-jet multiplicity sample, dominated by multi-jet QCD events, was used to extract an event weight as a function of ΔR_{bb} . The cross section changed by $< 15\%$ by including these weight factors.

The background sample was normalized to the candidate sample using the jj and bjj mass distributions. Specifically, the background dijet distribution was scaled to the candidate distribution so that the area with $M_{jj} < 65$ GeV was equal. This normalization factor was then adjusted downwards to avoid large negative deviations in the background-subtracted result. The normalization factor was reduced in 1% increments until the sum of the negative bins in the

TABLE I: Definition of loose, medium, and tight samples used in this analysis.

Requirement	Loose	Medium	Tight
aplanarity	none	$\mathcal{A} > 0.05$	$\mathcal{A} > 0.05$
centrality	none	$\mathcal{C} > 0.6$	$\mathcal{C} > 0.7$
sphericity	none	$\mathcal{S} > 0.2$	$\mathcal{S} > 0.5$
$\Delta R_{b\bar{b}}$	none	$\Delta R_{b\bar{b}} > 1$	$\Delta R_{b\bar{b}} > 2$

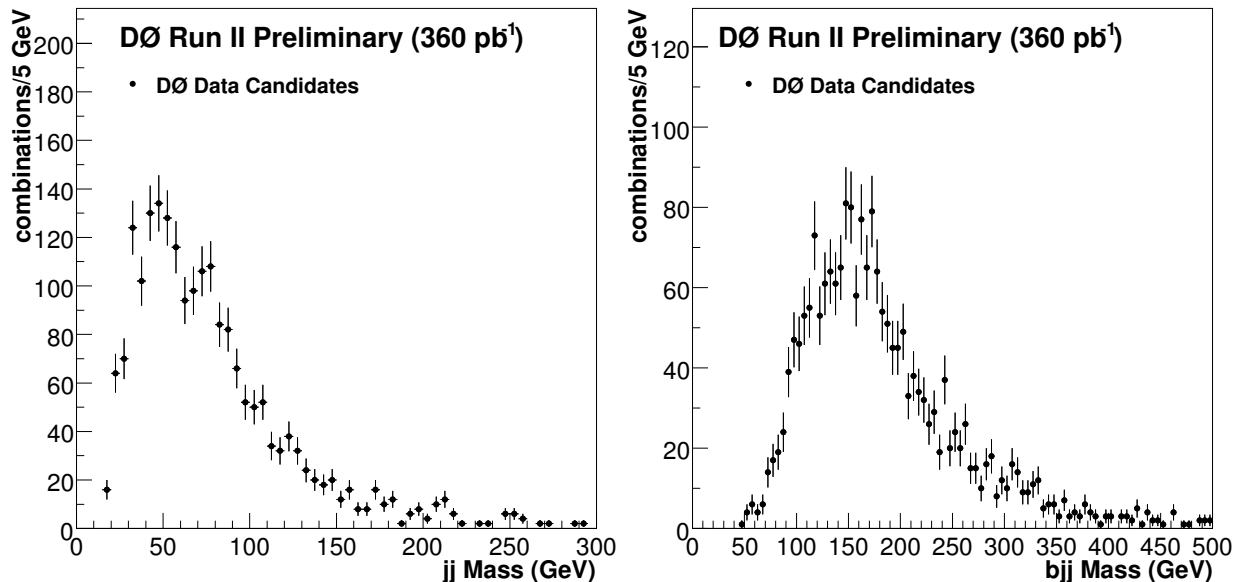


FIG. 1: Left: the dijet mass spectrum for all pairs of non- b tagged jets. Right: the three-jet mass spectrum for all combinations of one b -tagged jet and two non- b tagged jets.

bjj background-subtracted mass distribution was less than half the significance as follows:

$$\frac{1}{2} \sum_{i=1}^{\#bins} \left(|N_{bjj}^{\text{signal}}(i)| - N_{bjj}^{\text{signal}}(i) \right) \leq \frac{1}{2} \frac{N_{bjj}^{\text{signal}}}{\sqrt{N_{bjj}^{\text{candidates}}}}.$$

The jj and bjj mass distributions are shown in Figs. 2 and 3 with overlaid, normalized, background samples. The candidate distributions are significantly above background in the W -boson and t -quark mass ranges, respectively.

The PYTHIA v6.2 [7, 8] Monte Carlo event generator (with Tune A) was used to determine the efficiency for identifying $t\bar{t}$ in the multi-jet decay channel. The top quarks, generated with $m_t = 175$ GeV, were decayed into Wb with the W bosons decayed inclusively into quarks and leptons according to the predicted Standard Model branching fractions. EVTGEN [9] and TAUOLA [10] were used to decay heavy mesons and τ leptons respectively. Samples were processed through the full simulation chain. Jets were then additionally smeared in energy to improve agreement with the measured resolution and some jets were removed based on the probability to reconstruct a jet. The efficiencies associated with the identification of a b jet were adjusted to match those of the data [6]; the resulting scale factor was $S_{\text{SVT}} = 0.62 \pm 0.11$. The absolute jet energy scale in the Monte Carlo was scaled by $1.05^{+0.07}_{-0.05}$ so that the position of the W mass peak in the dijet decay mode agreed between data and Monte Carlo.

The background-subtraction technique described above is potentially biased as it could possibly subtract signal contributions at low mass. The fraction of the signal that survived this procedure, ϵ_{SB} , was determined with the $t\bar{t}$ Monte Carlo sample. The data background shapes, normalized to the ratio of the data and Monte Carlo luminosities, were added to the Monte Carlo signal distributions, then subtracted back out through the background procedure. ϵ_{SB} was defined as the fraction of events that survived the background subtraction and was $\approx 80\%$. Adjustments by up to 50% in the background normalization changed the cross section by $< 4\%$. The background-subtracted Monte Carlo mass distributions are compared to the background-subtracted data in Figs. 4 and 5.

The cross section for the inclusive production of $t\bar{t}$ was defined as

$$\sigma_{t\bar{t}} = \frac{1}{\mathcal{L}} \frac{(N^{\text{candidates}} - N^{\text{background}})}{\epsilon_{t\bar{t}} \epsilon_{SB} S_{\text{SVT}}}.$$

$N^{\text{candidates}}$ was the number of candidates in the sample; $N^{\text{background}}$ was the number of background events normalized by the procedure described above. The selection efficiency, $\epsilon_{t\bar{t}}$, was determined from the signal Monte Carlo sample. Values for these quantities, and the computed cross sections, are presented in Table II.

The background-subtracted results are compared with expectations from PYTHIA in Fig. 6. Additionally, in Figs. 7 and 8, comparisons between the candidates, background, and signal Monte Carlo are presented in aplanarity, sphericity, H_T , centrality, ΔR_{bb} , m_{bb} , p_{Tb} , and p_{Tjj} . The signal sample was normalized to the measured cross section.

TABLE II: Cross section for the inclusive production of pairs of top quarks as a function of topological requirements. Only statistical uncertainties are shown.

Sample Definition	$N^{\text{candidates}}$	$N^{\text{background}}$	ϵ^{SB} (%)	$\epsilon_{t\bar{t}}$ (%)	$\sigma_{t\bar{t}}$ (pb)
loose	173 ± 13	140.4 ± 0.8	80	1.51 ± 0.03	12.1 ± 4.9
medium	86 ± 9	60.7 ± 0.5	82	1.17 ± 0.02	11.8 ± 4.3
tight	14 ± 4	5.6 ± 0.1	79	0.37 ± 0.01	12.9 ± 5.8

TABLE III: Contributions to the systematic uncertainty associated with the $t\bar{t}$ cross section measurement.

Source	Uncertainty (%)
background model & subtraction	± 25
b ID scale factor	± 18
jet energy scale	± 15
Monte Carlo simulation	± 10
trigger	$^{+12}_{-3}$
luminosity	± 6.5
total	± 38

The major systematic uncertainties associated with the cross section measurement are shown in Table III and were dominated by signal and background modeling and the jet energy scale. The largest systematic uncertainty was due to the background modeling and subtraction ($\pm 25\%$). This uncertainty was estimated primarily by adjusting the criteria used in normalizing the background to the candidate distributions.

The cross section, taken from the loose sample, is 12.1 ± 4.9 (stat.) ± 4.6 (sys.) pb assuming $m_t = 175$ GeV. The dependence of the cross section on the top mass was about $-0.15(m_t - 175)$ pb/GeV. The inclusive production of $t\bar{t}$ has been calculated to NLO in α_s with additional NNLO soft-gluon corrections as 6.77 ± 0.42 (kinematic) ± 0.20 (scale) ± 0.45 (PDF) pb at $m_t = 175$ GeV [11, 12]. The measured integrated cross section is consistent with this Standard Model expectation. Background-subtracted distributions binned in the t -quark p_T , the $t\bar{t}$ mass and p_T , and the $\Delta\phi$ between the top quarks compared reasonably with results from the PYTHIA simulation.

We thank the staffs at Fermilab and collaborating institutions, and acknowledge support from the DOE and NSF (USA); CEA and CNRS/IN2P3 (France); FASI, Rosatom and RFBR (Russia); CAPES, CNPq, FAPERJ, FAPESP and FUNDUNESP (Brazil); DAE and DST (India); Colciencias (Colombia); CONACyT (Mexico); KRF and KOSEF (Korea); CONICET and UBACyT (Argentina); FOM (The Netherlands); PPARC (United Kingdom); MSMT (Czech Republic); CRC Program, CFI, NSERC and WestGrid Project (Canada); BMBF and DFG (Germany); SFI (Ireland); Research Corporation, Alexander von Humboldt Foundation, and the Marie Curie Program.

-
- [1] V. M. Abazov et al. (DØ Collaboration) (2005), physics/0507191.
 - [2] S. Abachi et al. (DØ Collaboration), Nucl. Instrum. Meth. **A338**, 185 (1994).
 - [3] V. M. Abazov et al., Nucl. Instrum. Meth. **A552**, 372 (2005).
 - [4] T. Edwards et al. (DØ Collaboration), FERMILAB-TM-2278-E.
 - [5] G. C. Blazey et al., hep-ex/0005012.
 - [6] V. M. Abazov et al. (DØ Collaboration), Phys. Lett. **B626**, 35 (2005).
 - [7] T. Sjostrand et al., Comput. Phys. Commun. **135**, 238 (2001).
 - [8] T. Sjostrand, L. Lonnblad, and S. Mrenna (2001), hep-ph/0108264.
 - [9] D. J. Lange, Nucl. Instrum. Meth. **A462**, 152 (2001).
 - [10] P. Golonka et al. (2003), hep-ph/0312240.
 - [11] N. Kidonakis and R. Vogt, Phys. Rev. **D68**, 114014 (2003).
 - [12] M. Cacciari et al., JHEP **04**, 068 (2004), hep-ph/0303085.

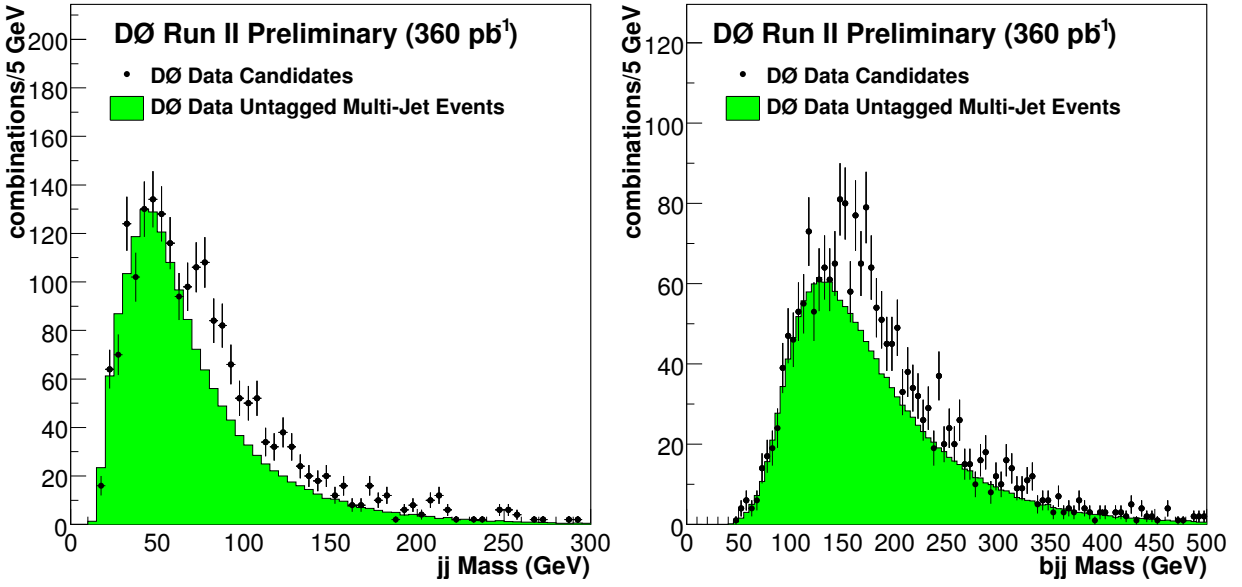


FIG. 2: Left: the dijet mass spectrum for all pairs of non- b tagged jets. Right: the three-jet mass spectrum for all combinations of one b -tagged jet and two non- b tagged jets. The green-shaded histogram overlaid on the data points is the distribution from the background sample.

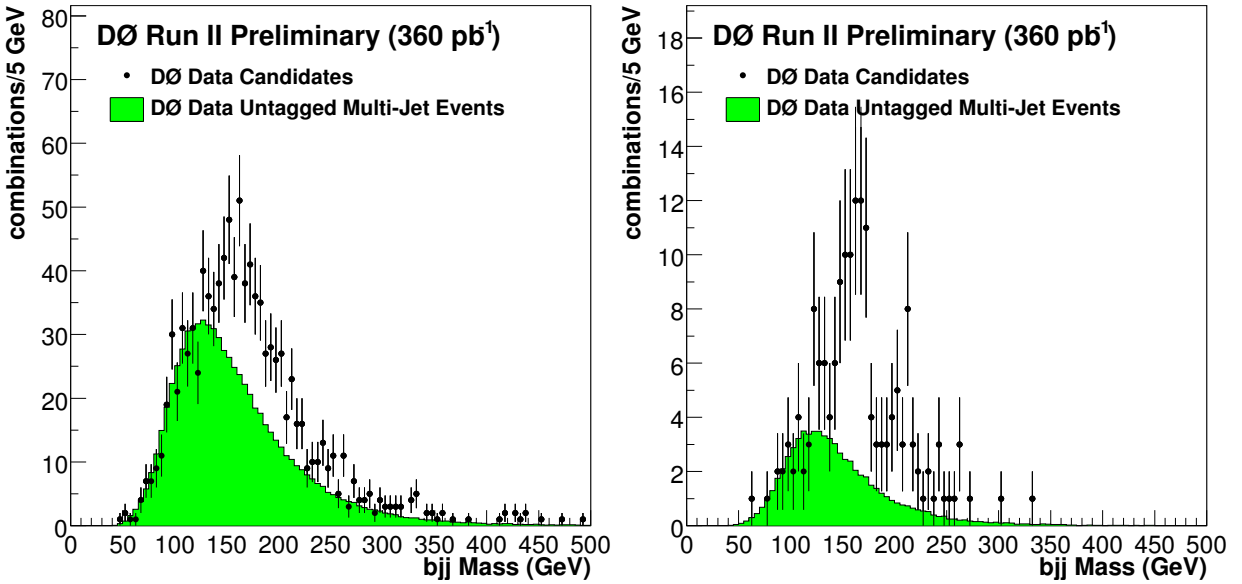


FIG. 3: Three-jet mass distributions for Left) the medium sample and Right) the tight sample. The green-shaded histogram overlaid on the data points is the distribution from the background sample.

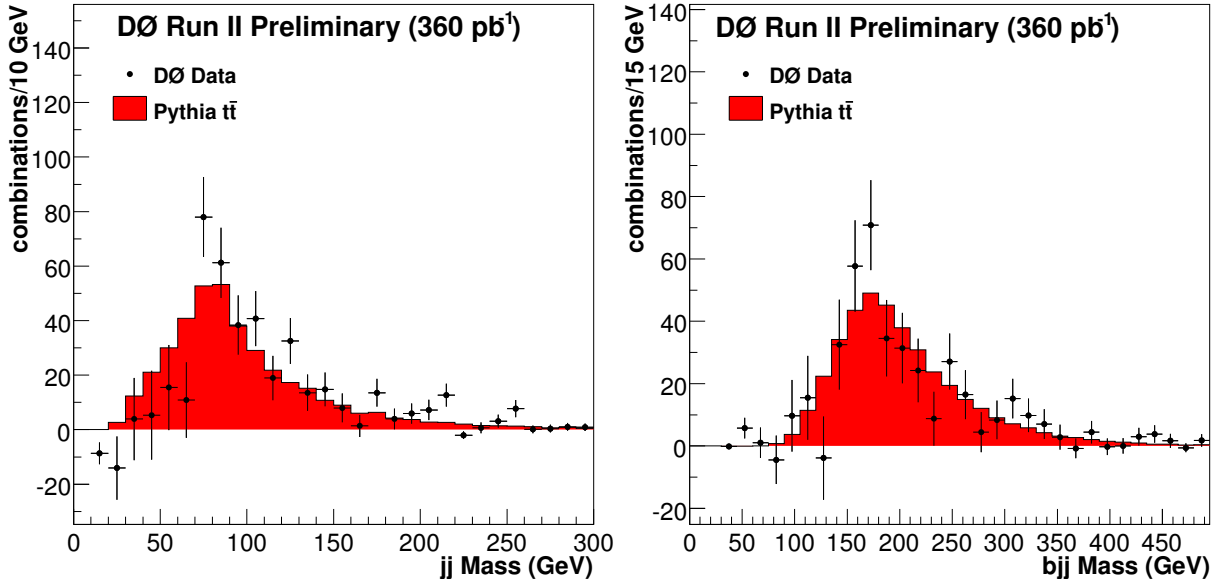


FIG. 4: Left: the dijet mass spectrum for all pairs of non- b tagged jets. Right: the three-jet mass spectrum for all combinations of one b -tagged jet and two non- b tagged jets. The red-shaded histograms overlaid on the background-subtracted data points are the distributions from the PYTHIA signal sample.

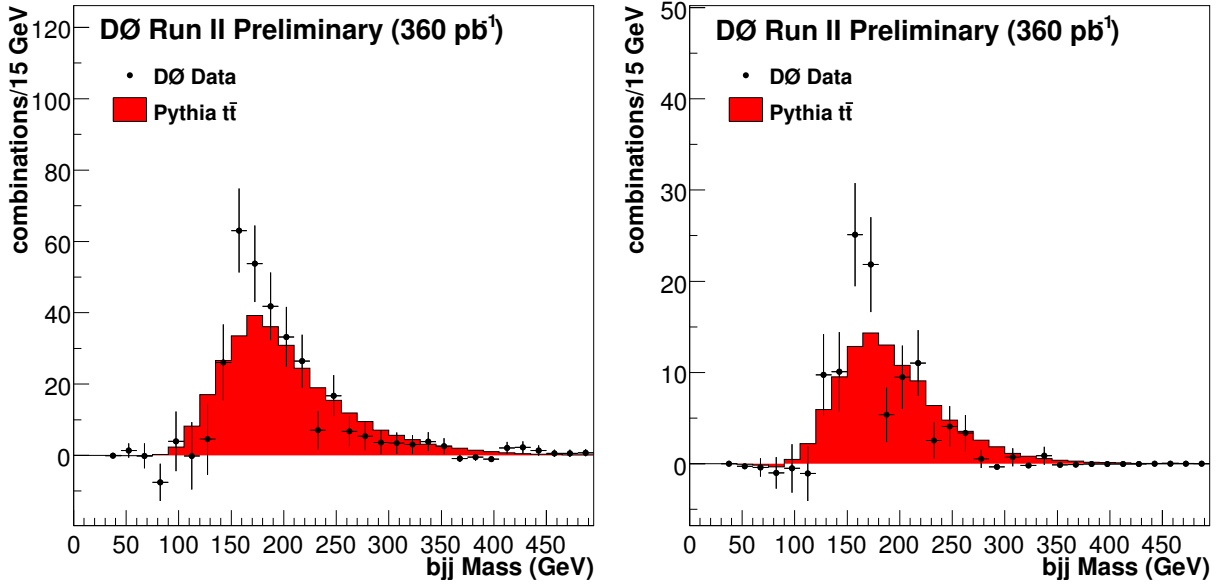


FIG. 5: Three-jet mass distributions for Left) the medium sample and Right) the tight sample. The red-shaded histograms overlaid on the background-subtracted data points are the distributions from the PYTHIA signal sample.

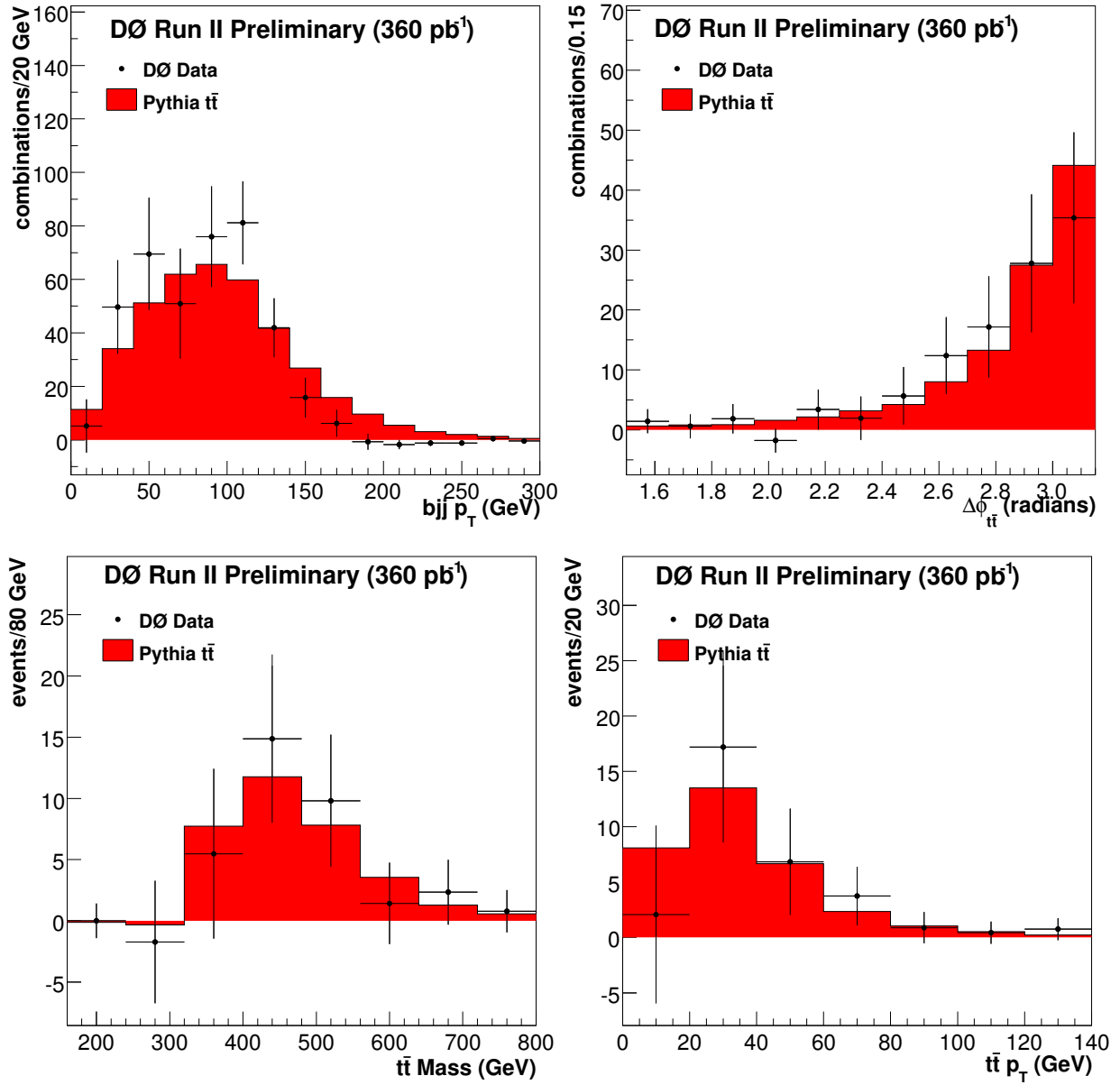


FIG. 6: Top-Left: top quark p_T distribution. Top-Right: $\Delta\phi$ between the top quarks. Bottom-Left: mass of the $t\bar{t}$ system. Bottom-Right: p_T of the $t\bar{t}$ system. Points are the background-subtracted data; the red histogram is the expectation from PYTHIA.

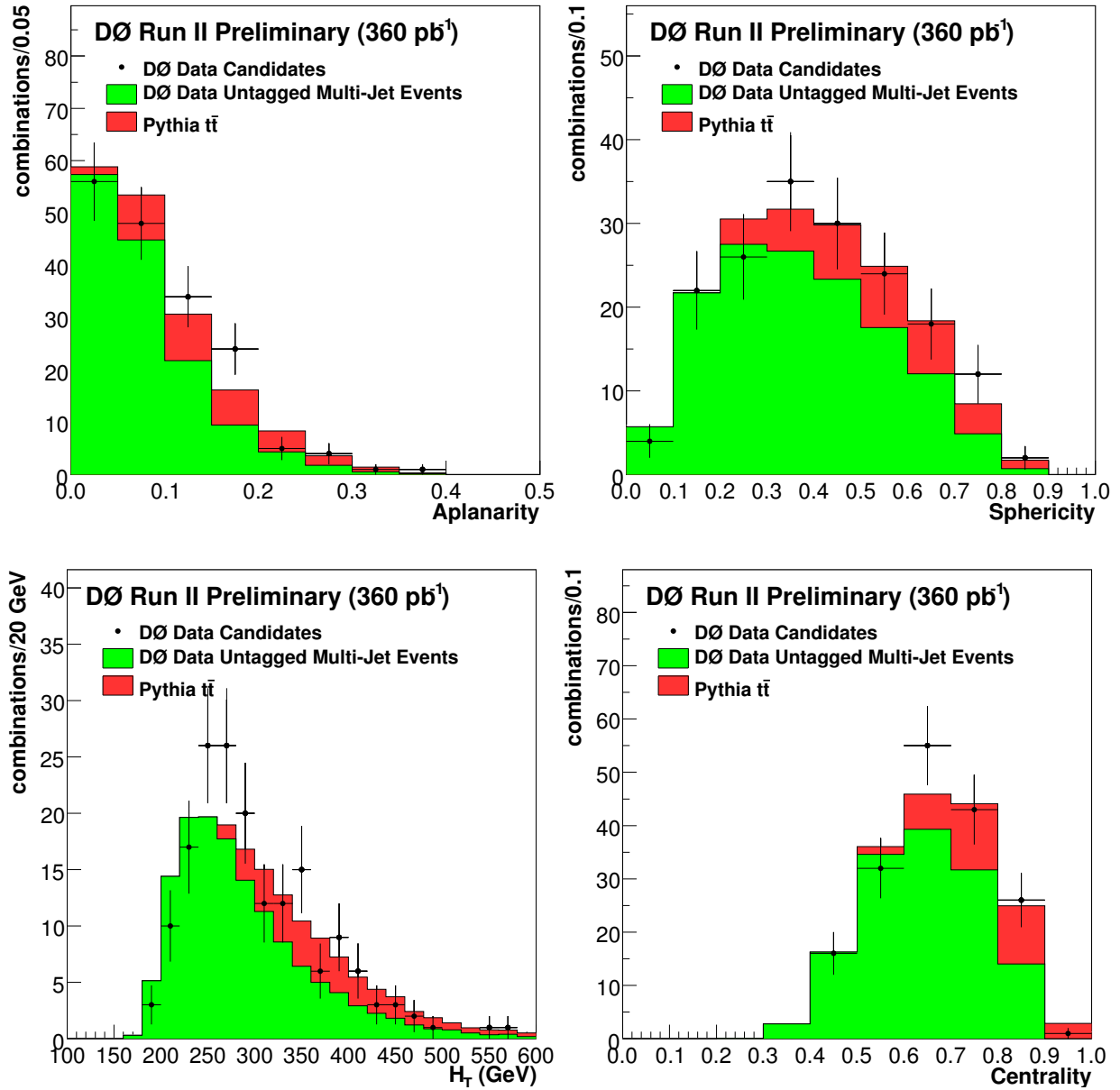


FIG. 7: Top-Left: aplanarity. Top-Right: sphericity. Bottom-Left: H_T . Bottom-Right: centrality. The red-shaded histograms (dark) are the distributions from the PYTHIA signal sample. The green-shaded histograms (light) are the distributions from the background sample.

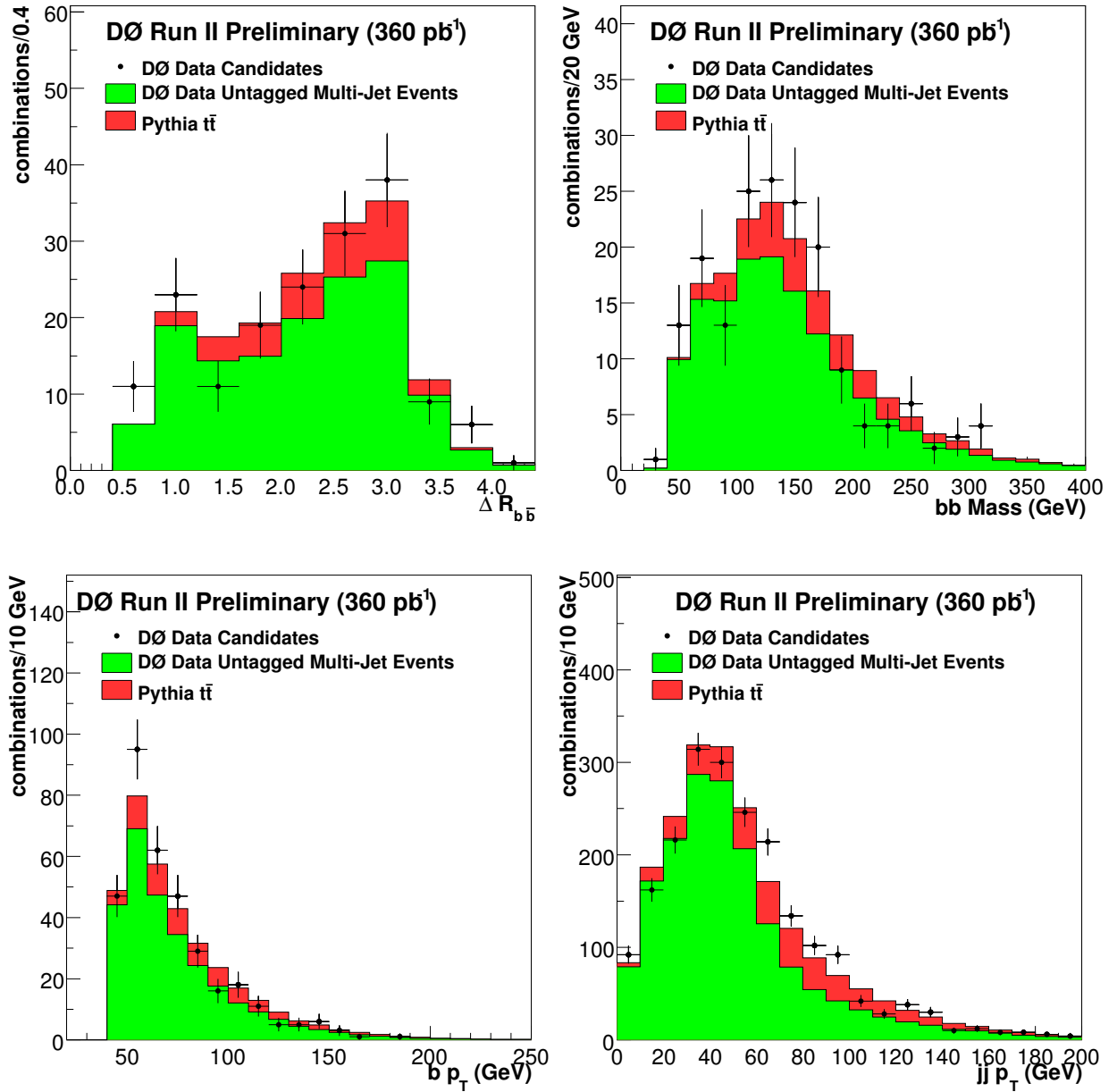


FIG. 8: Top-Left: ΔR_{bb} . Top-Right: mass of the bb pair. Bottom-Left: b jet p_T . Bottom-Right: dijet p_T . Distributions from the loose $6j$ base sample. The red-shaded histograms (dark) are the distributions from the PYTHIA signal sample. The green-shaded histograms (light) are the distributions from the background sample.